

1 **Tracking the temporal variation of COVID-19 surges through wastewater-based**  
2 **epidemiology during the peak of the pandemic: a six-month long study in Charlotte, North**  
3 **Carolina**

4 Authors: Visva Bharati Barua<sup>a\*</sup>, Md Ariful Islam Juel<sup>a\*</sup>, A. Denene Blackwood<sup>b</sup>, Thomas  
5 Clerkin<sup>b</sup>, Mark Ciesielski<sup>b</sup>, Adeola Julian Sorinolu<sup>a</sup>, David A. Holcomb<sup>c</sup>, Isaiah Young<sup>a</sup>, Gina  
6 Kimble<sup>d</sup>, Shannon Sypolt<sup>d</sup>, Lawrence S. Engel<sup>c</sup>, Rachel T. Noble<sup>b</sup>, Mariya Munir<sup>a</sup>

7 <sup>a</sup>Department of Civil and Environmental Engineering, University of North Carolina Charlotte,  
8 9201 University City Boulevard, Charlotte, NC 28223, USA

9 <sup>b</sup>Institute of Marine Sciences, The University of North Carolina at Chapel Hill, Morehead City,  
10 NC 28557, USA

11 <sup>c</sup>Department of Epidemiology, Gillings School of Global Public Health, The University of North  
12 Carolina at Chapel Hill, Chapel Hill, NC 27599, USA

13 <sup>d</sup>Charlotte Water, 5100 Brookshire Blvd., Charlotte, NC 28216, USA

14 \* These authors contributed equally

15 Corresponding author: Dr. Mariya Munir ([mmunir@uncc.edu](mailto:mmunir@uncc.edu))

16

17 **ABSTRACT**

18 The global spread of SARS-CoV-2 has continued to be a serious concern after WHO declared  
19 the virus the causative agent of the coronavirus disease 2019 (COVID-19) a global pandemic.

20 Monitoring of wastewater is a useful tool for assessing community prevalence given that fecal  
21 shedding of SARS-CoV-2 occurs in high concentrations by infected individuals, regardless of  
22 whether they are asymptomatic or symptomatic. Using tools that are part of the wastewater-  
23 based epidemiology (WBE) approach, combined with molecular analyses, wastewater

24 monitoring becomes a key piece of information used to assess trends and quantify the scale and  
25 dynamics of COVID-19 infection in a specific community, municipality, or area of service. This  
26 study investigates a six-month long SARS-CoV-2 RNA quantification in influent wastewater  
27 from four municipal wastewater treatment plants (WWTP) serving the Charlotte region of North  
28 Carolina (NC) using both RT-qPCR and RT-ddPCR platforms. Influent wastewater was analyzed  
29 for the nucleocapsid (N) genes N1 and N2. Both RT-qPCR and RT-ddPCR performed well for  
30 detection and quantification of SARS-CoV-2 using the N1 target, while for the N2 target RT-  
31 ddPCR was more sensitive. SARS-CoV-2 concentration ranged from  $10^3$  to  $10^5$  copies/L for all  
32 four plants. Both RT-qPCR and RT-ddPCR showed a significant moderate to a strong positive  
33 correlation between SARS-CoV-2 concentrations and the 7-day rolling average of clinically  
34 reported COVID-19 cases using a lag that ranged from 7 to 12 days. A major finding of this  
35 study is that despite small differences, both RT-qPCR and RT-ddPCR performed well for  
36 tracking the SARS-CoV-2 virus across WWTP of a range of sizes and metropolitan service  
37 functions.

38 **Keywords:** SARS-CoV-2; wastewater; COVID-19; RT-qPCR; RT-ddPCR; wastewater-based  
39 epidemiology (WBE)

## 40 **1. Introduction**

41 The global pandemic “Coronavirus disease 2019 (COVID-19)”, as declared by the World Health  
42 Organization (WHO, 2020a), is caused by the virus given the name "Severe Acute Respiratory  
43 Syndrome Coronavirus 2" (SARS-CoV-2). The single-stranded ribonucleic acid (RNA) SARS-  
44 CoV-2 virus can infect individuals causing a range of symptoms, which can include life-  
45 threatening health complications on one end of the spectrum or a lack of symptoms  
46 (asymptomatic carriers). Interestingly, both symptomatic and asymptomatic individuals have the

47 potential to spread the virus to others in the population (Bai et al., 2020). This makes tracking  
48 infected individuals and implementing appropriate preventative measures difficult.  
49 During the onset of the COVID-19 pandemic, clinical testing was restricted primarily to  
50 individuals exhibiting life-threatening health complications owing to limited COVID-19 clinical  
51 testing kits (CDC, 2020). Thus, many asymptomatic and even symptomatic individuals were  
52 excluded from the COVID-19 case counts when public health decisions were made (Murakami  
53 et al., 2020) during the early stages of the pandemic. Although later stages of the pandemic have  
54 included testing of asymptomatic individuals, for either surveillance or screening, testing has  
55 been neither comprehensive nor representative. Therefore, clinical testing has been valuable for  
56 managing isolation and quarantine of individuals, but the pooling of clinical testing data has  
57 limited utility for understanding overall trends or inferring the prevalence of infection in entire  
58 communities/counties.

59 Monitoring of SARS-CoV-2 in wastewater influent from municipal wastewater treatment plants  
60 (WWTP) has been demonstrated to be a useful tool for predicting clinical outcomes for whole  
61 communities (Agrawal et al., 2021; Ahmed et al., 2021; Hillary et al., 2021; Saguti et al., 2021).  
62 Wastewater influent is an aggregate measure of the prevalence of infection in a community,  
63 particularly for viral, bacterial and protozoan pathogens that are carried in fecal material. SARS-  
64 CoV-2 RNA concentration in wastewater influent has not only been correlated with reported  
65 COVID-19 cases, but they have been predictive of the clinical testing outcomes in communities  
66 sometimes with as much as a 6 to 14 day lead time (Kumar et al., 2021; Peccia et al., 2020).

67 Monitoring of influent wastewater has revolutionized the tracking of pathogens in municipalities,  
68 communities, and even small-scale systems such as dormitories and workplaces. Monitoring of  
69 SARS-CoV-2 in wastewater influent includes virus being shed from symptomatic, clinically

70 diagnosed, and asymptomatic individuals. This area of active research will yield beneficial  
71 information for guiding public health decisions.

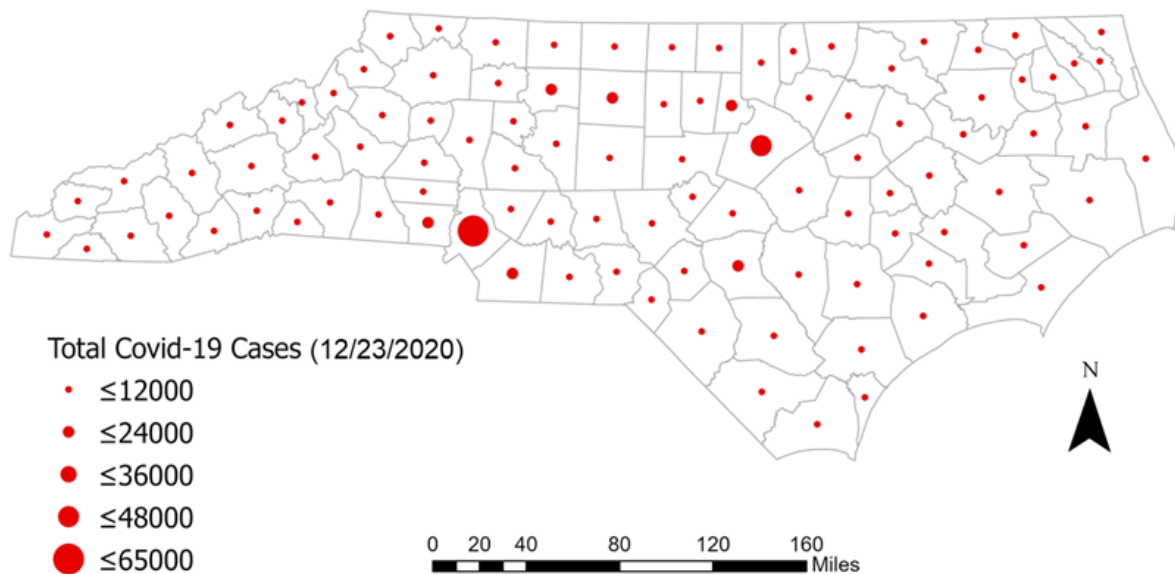
72 WBE is a potential approach for understanding the proliferation of SARS-CoV-2 within a  
73 community as the viral RNA is shed by infected individuals into wastewater (Hasan et al., 2021;  
74 Hemalatha et al., 2021). Aoust et al. (2021) reported that the surges in SARS-CoV-2 RNA in  
75 wastewater were observed 48 h prior to clinical testing and 96 h prior to hospitalization.

76 Wastewater sampling captures the community signal comprising both symptomatic and  
77 asymptomatic individuals (Bivins et al., 2020; Peccia et al., 2020), suggesting the value of WBE  
78 as an impartial surveillance system at a community level when making public health decisions.

79 To date, numerous studies have documented the detection of SARS-CoV-2 in the influent of  
80 municipal wastewater i.e., Ahmed et al. (2020); Albastaki et al. (2021); Bertrand et al. (2021);  
81 Gonçalves et al. (2021); Kumar et al. (2020); to name a few but their study period ranged from  
82 only 15-30 days. Weidhaas et al. (2021) articulated the need for a meticulous WBE study for  
83 prolonged periods in localities with lower and higher COVID-19 cases to identify the  
84 relationship between concentrations of SARS-CoV-2 RNA in municipal wastewater and rates of  
85 COVID-19 cases in the corresponding communities.

86 This manuscript details a six-month long WBE study for the surveillance of SARS-CoV-2 in the  
87 influent municipal wastewater of Charlotte, North Carolina (NC). The number of clinical cases  
88 of COVID-19 in Mecklenburg County, where Charlotte is located, was highest among all the  
89 counties of NC. The most populous city in NC, Charlotte includes the Charlotte Douglas  
90 International Airport. By December 2020, the number of COVID-19 cases was reported to be  
91 greater than 65,000 in Mecklenburg County (North Carolina Department of Health and Human  
92 Services, NCDHHS). Fig. 1 shows Mecklenburg County where Charlotte is located to report the

93 highest number of COVID-19 cases in NC. As of September 11, 2021, Mecklenburg County  
94 leads the state in total reported COVID-19 cases with 141,000.



95  
96 **Fig.1.** Map showing the total number of clinically reported COVID-19 cases, county-wise, in the  
97 state of NC for the duration of this study (Prepared by the software ArcGIS Pro).

98  
99 To date, SARS-CoV-2 wastewater surveillance studies have mostly employed RT-qPCR for viral  
100 quantification (Ahmed, Angel, et al., 2020; Chik et al., 2021; Gerrity et al., 2021; Haramoto et  
101 al., 2020; Medema et al., 2020; Nemudryi et al., 2020; Peccia et al., 2020; Randazzo et al., 2020;  
102 Sherchan et al., 2020; Westhaus et al., 2021; Wurtzer et al., 2020; Zhao et al., 2021) rather than  
103 RT-ddPCR (Gonzalez et al., 2020; Gonzalez et al., 2021). Only a few research groups have used  
104 both RT-qPCR and RT-ddPCR quantification (Aoust, Graber, et al., 2021; Ciesielski et al., 2021;  
105 Dumke et al., 2021; Graham et al., 2021). The study conducted by both Graham et al. (2021) and  
106 Aoust et al. (2021) focussed on RT-qPCR and RT-ddPCR quantification for solids from WWTP,  
107 while Dumke et al. (2021) targeted E and S genes to quantify SARS-CoV-2 in wastewater.  
108 Ciesielski et al. (2021) performed an interlaboratory validation study of 60 samples comparing  
109 RT-qPCR to RT-ddPCR quantification. The aim of this study was to (a) compare the utilization

110 of two different molecular quantification platforms to identify the changing aspects of SARS-  
111 CoV-2 viral concentration in the wastewater influent from four WWTP serving Charlotte, North  
112 Carolina (NC) for six months, and (b) to correlate wastewater concentration (quantified by both  
113 RT-qPCR and RT-ddPCR) with clinical surveillance data of SARS-CoV-2 infection.

## 114 **2. Methodology**

### 115 **2.1 Sample collection**

116 24-h flow-weighted composite samples of influent wastewater were initially collected every  
117 Wednesday starting on June 24, 2020, from four WWTP (A, B, C, and D) in Charlotte, North  
118 Carolina. Wastewater samples were collected in the morning between 7:00-8:45 am in sterile 1L  
119 Nalgene bottles. Following collection, the wastewater samples were heat pasteurized for 40  
120 minutes at 75°C in accordance with the Institutional Biosafety Committee's mandatory protocol for  
121 the protection of laboratory personnel (WHO, 2020b). Heat pasteurized duplicate samples from  
122 each WWTP were transported to the laboratory in coolers packed with ice. Deionized water in a  
123 1 L Nalgene sample collection bottle was used as a field blank. The field blank was exposed to  
124 the same environment and transported to the laboratory in coolers packed with ice along with the  
125 wastewater samples. The collected samples were processed immediately after reaching the  
126 laboratory. A recent study conducted by Pecson et al. (2021) observed that SARS-CoV-2  
127 quantitation was slightly higher in pasteurized samples after recovery correction. Sample  
128 collection increased to twice a week, on Monday and Wednesday during November and  
129 December 2020. Monday sampling represented the 24 h composite sample beginning on Sunday  
130 through Monday while Wednesday sampling represented the 24 h composite sample beginning  
131 on Tuesday through Wednesday. A total of 115 wastewater samples were collected during 31  
132 sampling events. Data from two sampling events were not included in this reported dataset

133 because the PBS blank demonstrated cross-contamination of the samples. The characteristics of  
134 each of the WWTP have been provided in Table1.

135 **Table 1:** Wastewater Treatment Plant (WWTP) characteristics.

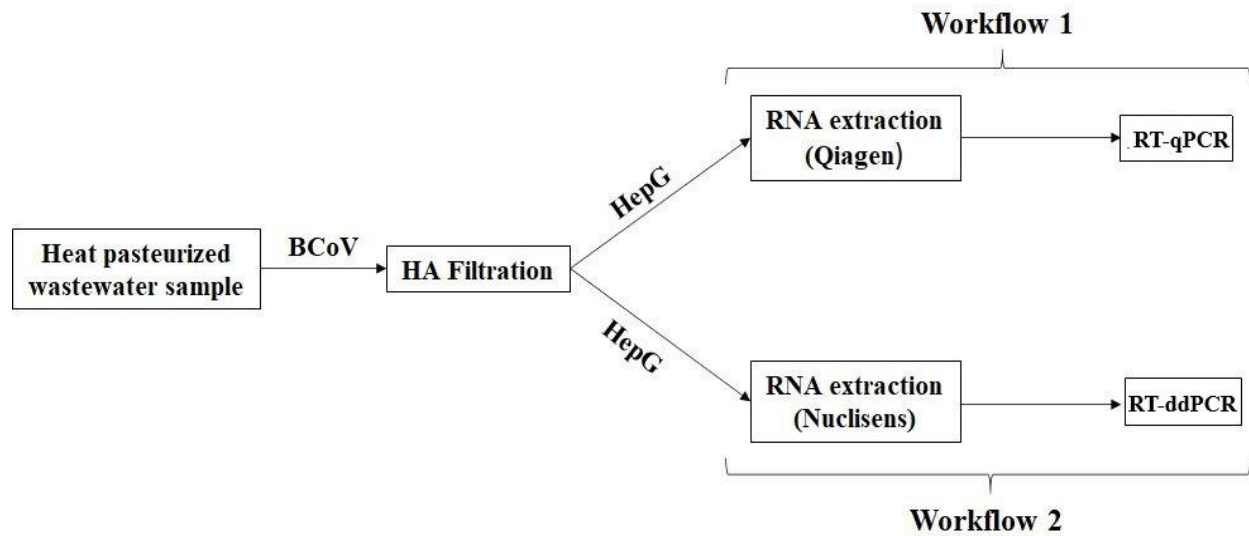
WWTP	A	B	C	D
<b>Permitted Flow</b>	12 MGD	12 MGD	20 MGD	100,000 GPD
<b>Average Daily Flow</b>	9.6 MGD	5.5 MGD	14.6 MGD	46,650 GPD
<b>Estimated Population Served</b>	120,001	68,685	182,501	Less than 1000
<b>Service area</b>	3 Permitted Significant Industrial Users, Major Hospital served, University Campus	All residential and commercial, Major Hospital	14 Permitted Significant Industrial Users, Major Hospitals, Serves part of Uptown Charlotte	Package Plant Services Residential Community Only

136

## 137 **2.2 Sample concentration**

138 6300 copies/ $\mu$ L of Bovine Coronavirus (BCoV, ValleyVet Supply, Marysville, KS) were spiked  
139 into the wastewater sample before concentration as overall process control. Wastewater samples  
140 were adjusted to a pH of 3.5-4 using 10M HCl, followed by the addition of 2.5 M  $MgCl_2 \cdot 6H_2O$   
141 to achieve a final concentration of 25 mM  $MgCl_2 \cdot 6H_2O$  (Ahmed, Bertsch, et al., 2020;  
142 Cashdollar and Wymer, 2013). Using a disposable filter funnel fitted with a 47 mm dia. 0.45  $\mu$ m  
143 type HA Filter (Millipore, Bedford MA), 20 mL of each wastewater sample was concentrated  
144 using a vacuum filtration manifold and was filtered to dryness. Negative process control or  
145 Method Blank (MB) consisting of 1X phosphate buffered saline (PBS) was filtered during each  
146 of the sample processing events using a new sterile filter funnel and type HA electronegative  
147 filter (Ciesielski et al., 2021). After wastewater concentration, the filter was placed in individual

148 2 mL microcentrifuge tubes. The process was repeated 8 times for each wastewater sample. One  
149 filter was used for Workflow 1, one for Workflow 2, (Fig. 2) and the others were archived at -  
150 80°C for future analyses. For workflow 1 the filter was suspended in the AVL buffer for RNA  
151 extraction.



152  
153 **Fig. 2.** Showing the two different workflows performed to quantify SARS-CoV-2 in the influent  
154 wastewater.

### 155 **2.3 Workflow 1**

#### 156 **2.3.1 Viral RNA extraction**

157 The filters with concentrated samples were suspended in 1000  $\mu$ L of AVL lysis buffer with  
158 carrier RNA and spiked with 15,600 copies of armored Hepatitis G (Hep G) (p/n 42024  
159 Asuragen, Austin, TX). Samples were then vortexed and incubated at room temperature for 10  
160 minutes to facilitate viral recovery from the filter surface (Gibas et al., 2021; Juel et al., 2021).  
161 QIAamp® Viral RNA Mini Kit (Qiagen, Germantown, Maryland, USA) was used following the  
162 manufacturer's instructions for viral RNA extraction where the amount of the lysed sample was  
163 200  $\mu$ L with a final elution volume of 60  $\mu$ L of viral RNA extract.

#### 164 **2.3.2 Detection and quantification using RT-qPCR**



165 Detection and quantification of SARS-CoV-2 viral RNA in wastewater were performed by one-  
166 step RT-qPCR on a CFX Connect thermocycler (Bio-Rad, Hercules, CA) utilizing the 2019-  
167 nCoV CDC RUO Kit (Integrated DNA Technologies) targeting the nucleocapsid genes (N1 and  
168 N2) (Table S1). The reaction mixture comprised a total volume of 20  $\mu$ L containing 5  $\mu$ L  
169 extracted RNA template, 10  $\mu$ L iTaq universal probes reaction mix (Bio-Rad), 0.5  $\mu$ L iScript  
170 reverse transcriptase (Bio-Rad), 1.5  $\mu$ L (500 nM) primers along with a (125 nM) probe and 3  $\mu$ L  
171 of nuclease-free water. The thermocycling conditions employed were 25°C for 2 min, 50°C for  
172 15 min, 95°C for 2 min followed by 45 cycles of amplification including denaturation at 95 °C  
173 for 3 secs and extension at 55 °C for 30 secs (CDC RT-qPCR panel 2020). Synthetic, single-  
174 stranded SARS-CoV-2 RNA (Twist Bioscience, San Francisco, CA) was used as a positive  
175 control. No template control (NTC) in triplicate was included with every run, where the RNA  
176 template was replaced with nuclease-free water, to determine if the mastermix was contaminated  
177 and if there was non-specific amplification during the later amplification cycles. Each sample  
178 was analyzed in triplicate, including the positive control and NTC reactions on each RT-qPCR  
179 run. RT-qPCR runs were analyzed by Bio-Rad CFX Manager software version 3.1 (Bio-Rad  
180 Laboratories).

### 181 ***2.3.3 Quality Control (QC) Parameters***

182 Precise QC metrics were considered to assess the detection sensitivity of CDC recommended N1  
183 and N2 assays for both workflow 1 (RT-qPCR) and workflow 2 (RT-ddPCR). QC was taken into  
184 consideration throughout the whole study to avoid ambiguous interpretation of the obtained  
185 results. The positive and negative controls used during each of the steps for both the workflows  
186 (1 and 2) were in accordance with MIQE (Bustin et al., 2009) and the digital MIQE (dMIQE

187 Group, 2020) guidelines. The detailed quality control and the criteria for data evaluation  
188 implemented has been provided below;

#### 189 ***2.3.3.1 Process Control***

190 BCoV was spiked into wastewater samples as a proxy for SARS CoV-2, which could be  
191 measured throughout the extraction and RT-qPCR process. 6300 copies of BCoV vaccine was  
192 spiked per mL of wastewater. The initial titer of BCoV vaccine was quantified by RT-ddPCR  
193 prior to spiking. The average BCoV recovery for each of the WWTP was observed to be 21-  
194 31%.

#### 195 ***2.3.3.2 Extraction control***

196 15,600 copies of armored hepG were spiked into the lysis buffer before the RNA extraction  
197 process to check the quality of the extracted RNA. The initial concentration of the armored hepG  
198 was determined by ddPCR after heat treatment at 75°C for 3 minutes to remove the protein coat  
199 surrounding the HepG RNA sequence. The average HepG recovery for each of the WWTP was  
200 observed to be 38-44%.

#### 201 ***2.3.3.3 Standard Curve***

202 Single-stranded RNA from Twist Bioscience was extracted in the same manner as wastewater  
203 influent samples. The RNA standard was quantified using RT-ddPCR prior to extraction. 10-  
204 fold serial dilution was performed with the extracted RNA over four orders of magnitude for  
205 generating N1 and N2 standard curves. Detailed information has been provided in the  
206 supplementary file (Fig. S1). The amplification efficiency was 90% for both N1 and N2 assay  
207 with an R<sup>2</sup> value of 0.998 and 0.997, respectively which was within the acceptable range as  
208 specified in MIQE guidelines (Bustin et al., 2009).

#### 209 ***2.3.3.4 Limit of Detection***

210 To avoid false positives and provide precise quantification, the limit of detection (LoD) for the  
211 assay was determined by running an extended series of dilutions of the RNA based SARS-CoV-2  
212 positive control (Twist Bioscience) in six replicates with as few as 1 copy/reaction (three-fold  
213 dilution series towards the lower end). The threshold cycle at which signals were observed for all  
214 the three replicates with a standard deviation less than 1 was considered to be the Cq of LoD  
215 ( $Cq_{LoD}$ ). Cq values of 37.07 and 37.78 for N1 and N2 assays, respectively were converted to  
216 copies per reaction using the equation (1) to get the LoD for the assay.

217  $X_0 = E_{AMP}^{(b-Cq)} \dots\dots\dots (1)$

218 Where,  $E_{AMP}$  represents exponential amplification value of RT-qPCR assay, evaluated as  $E_{AMP} =$   
219  $10^{-1/m}$ ,  $b$  represents the intercept and  $m$  represents the slope. The LoD for workflow 1 was  
220 determined as 3000 copies/L of wastewater for both targets.

221 **2.3.3.5 Inhibition**

222 The dilution method was used for the determination of the RT-qPCR inhibition (Graham et al.,  
223 2021). A dilution series of 1:1, 1:2, 1:5 and 1:10 was performed on a subset of samples (n=10)  
224 for assessing inhibition. If the diluted sample showed a more than 1 Cq difference between the  
225 actual and theoretically expected change in Cq, then the undiluted samples were considered  
226 inhibited. There was no inhibition observed for the N1 target but there was with N2. A dilution  
227 1:2 was selected to continue inhibition testing as further dilution resulted in Cq values beyond  
228 LoD or as non-detectable and the quantification data was updated accordingly.

229 **2.3.3.6 Other Criteria for QC and data evaluation:**

- 230 • RNA extraction and master mix preparation for molecular quantification was conducted  
231 in two different biosafety cabinets in two separate laboratories next to each other to  
232 reduce contamination potential.

- 233       • RNA samples showing very poor overall recovery (below 2%) compared to the average  
234       recovery (23%) were re-extracted and re-quantified.
- 235       • Samples were considered positive when a minimum of two out of three replicates showed  
236       amplification above LoD for N1 and N2 assay.

## 237   **2.4 Workflow 2**

### 238   **2.4.1 Viral RNA extraction**

239   Frozen filters containing the concentrated sample were shipped on dry ice and stored at -80°C  
240   until analysis. The filter containing the concentrated sample was placed in 1mL of Nuclisens®  
241   easyMAG® Lysis Buffer (Biomerieux, Durham, NC) containing approximately 900 copies of  
242   armored HepG and incubated for a minimum of 10 minutes at room temperature. Lysis tubes  
243   were centrifuged for 1 minute at 13,000 x g and up to 950 µL of lysate transferred to a 96 well  
244   deep well plate (DWP). All samples, including controls, were extracted using NucliSens®  
245   EasyMAG reagents (Biomerieux, Durham, NC) on a KingFisher Flex (ThermoFisher, Waltham,  
246   MA) with a final elution volume of 100µL. KingFisher script is provided in the supplementary  
247   material (Table S7a).

### 248   **2.4.2 Detection and quantification using RT-ddPCR**

249   RT-ddPCR was utilized to quantify SARS-CoV-2 RNA copies targeting N1 and N2, described  
250   previously (Table S1), and utilizing a two-step reverse transcription and RT-ddPCR. Purified  
251   RNA was reverse transcribed using Superscript VILO IV MM (ThermoFisher Waltham, MA.).  
252   Briefly, 50µL of the eluate was combined with 20µL 5X VILO IV MM, 1µL (160 copies) mouse  
253   lung RNA (p/n R1334152-50 BioChain Newark, CA) and 29µL of DEPC water for a total  
254   reaction volume of 100 µL (Table S7a). Reverse transcription was performed on a C1000 deep  
255   block thermal cycler (BioRad) with the following conditions: 25°C for 10 minutes, 50°C for 10

256 mins, and 85°C for 5 minutes. 5 µL of cDNA was used for each RT-ddPCR reaction. A  
257 mastermix was created by the addition of forward and reverse primers (0.9µM final  
258 concentration) and for probes (0.25µM final concentration), 12.5µL of 2X Supermix for Probes  
259 (no dUTP, Bio-Rad), 5µL template, and nuclease-free water for a final volume of 25µL. A  
260 minimum of 4 no template controls (NTC), which substituted 5µL nuclease-free water for the  
261 template, were included in each run with every assay plate. Primers and probes were synthesized  
262 by LGC Biosearch Technologies (Novato, CA) except for Mouse ACTB exogenous control (Life  
263 Technologies ThermoFisher Scientific Waltham, MA). The concentration used in the assays is  
264 listed in S7b. Primers and probe sequences for the *gyrA* for inhibition control were kindly  
265 provided by John Griffith (SCCWRP) and have not been published. The inhibition probe was  
266 labeled with the HEX fluorophore and the RT-ddPCR assay was run as a duplex with all  
267 reactions performed in duplicate. Positive and negative controls were run on every assay plate.  
268 All assay conditions were previously optimized and established by the Noble Laboratory.  
269 Droplet generation was performed in accordance with manufacturer's instructions, and then  
270 droplets were amplified in a C1000 thermal cycler with the following temperature profile: 10  
271 min at 95°C for initial denaturation, 40 cycles of 94°C for 30 s, and 55°C for 60 s, followed by  
272 98°C for 10 min, with a ramp rate of 2°C per sec, then an indefinite hold at 12°C. After RT-  
273 ddPCR cycling was complete, the plate was placed in a QX200 instrument (Bio-Rad) and  
274 droplets were analyzed according to the manufacturer's instructions. Data acquisition and  
275 analysis were performed with QuantaSoft V1.74.0917 (Bio-Rad). The fluorescence amplitude  
276 threshold, distinguishing positive from negative droplets, was set manually by the analyst as the  
277 midpoint between the average baseline fluorescence amplitude of the positive and negative  
278 droplet cluster. The same threshold was applied to all the wells of one RT-ddPCR plate.

279 Measurement results of single RT-ddPCR wells were excluded on the basis of technical reasons  
280 in case that (i) the total number of accepted droplets was <10,000, or (ii) the average  
281 fluorescence amplitudes of positive or negative droplets were clearly different from those of the  
282 other wells on the plate. The numbers of positive and accepted droplets and concentration per  
283  $\mu\text{L}$  were transferred to an in-house developed spreadsheet to calculate the copy number per  
284 filtered volume. Replicate wells were merged, and a sample was considered positive only if  
285 there were three or more positive droplets and each well contained a minimum of 10,000  
286 droplets.

#### 287 ***2.4.3 Process Control***

288 BCoV was spiked into wastewater samples as a proxy for SARS CoV-2, which could be  
289 measured throughout the extraction and RT-qPCR process. The copy number of BCoV was  
290 quantified by RT-ddPCR prior to spiking. The filter was extracted utilizing the same viral RNA  
291 extraction kit as the influent wastewater samples. About 38-44% average BCoV recovery was  
292 observed for each of the WWTP.

#### 293 ***2.4.4 Extraction control***

294 Approximately 900 copies of armored HepG were spiked into the Lysis Buffer before the RNA  
295 extraction process to monitor the quality of the extracted RNA. Negative extraction controls  
296 (NECs) were included to verify the absence of cross-contamination and consisted of a blank HA  
297 filter processed under the same conditions as the other samples. The initial concentration of the  
298 armored HepG was determined by RT-ddPCR after heat treatment at 75°C for 3 minutes to  
299 remove the protein coat surrounding the HepG RNA sequence. The average HepG recovery for  
300 all the WWTP was found to be 17.3 - 29.8%.

#### 301 ***2.4.5 Inhibition control***

302 PCR inhibition was measured by the addition of a halophilic archaeon containing 160 copies of  
303 the *gyrA* gene into the mastermix. The halophiles had been cultured, aliquots frozen at -20°C,  
304 and the concentration determined independently prior to the sample analysis. Inhibition was  
305 measured by the addition of exogenous cells and a sample was deemed inhibited if the difference  
306 of the expected versus the actual concentration differed by greater than 0.5 log (Table S6).

#### 307 ***2.4.6 Reverse transcription (RT) efficiency control***

308 162 copies of mouse lung total RNA were spiked into the reverse transcription master mix and  
309 the recovery was measured using a mouse ACTB assay (Life Technologies). Recovery was  
310 measured by dividing the concentration of the unknown sample by the negative extraction  
311 control and multiplying by 100 (Table S7b).

#### 312 ***2.4.7 N1 and N2 Standard***

313 Armored RNA Quant SARS-CoV-2 control, which encapsulates the in vitro transcribed RNA  
314 template in a protective protein coat and targets the SARS-CoV-2 viral nucleocapsid (N) region,  
315 was used as a positive control and run in duplicate for every set of reactions targeting N1 and  
316 N2.

#### 317 ***2.4.8 Limit of Detection, Limit of Quantification, and Limit of Blank***

318 For the determination of LoD using RT-ddPCR, the Limit of Blank (LoB) was elucidated from  
319 eight replicates of negative matrix samples derived from influent collected at multiple WWTP  
320 throughout eastern NC. The LOB was calculated as the mean concentration of all sixty-four  
321 replicates and the LOD was then calculated as two standard deviations beyond the defined LOB  
322 (Hayden et al., 2013). The LOQ was determined to be never less than 3 positive droplets no  
323 matter the number of merged wells, which for this study was two, resulting in 10 µL or 10% of

324 the RNA eluate and is equal to a concentration of 10 copies. The detailed LOB, LOD, and LOQ  
325 for N1 and N2 gene targets for RT-ddPCR has been provided in Table 2.

326 **Table 2:** LOB, LOD, and LOQ for N1 and N2 gene targets for RT-ddPCR.

	N1	N2
LOB (copies/L)	52.312	15.619
estimated LOD (copies/L)	1101.303	330.011
LOQ (copies/L)	1101.33	1000

327

### 328 **2.5 Recovery efficiency of BCoV and HepG**

329 The following formula was utilized for both workflow 1 and 2 to determine the recovery  
330 efficiency of BCoV and HepG;

$$331 \quad \text{Recovery efficiency}(\%) = \left( \frac{\text{Total copies recovered}}{\text{Total copies spiked}} \right) \times (100)$$

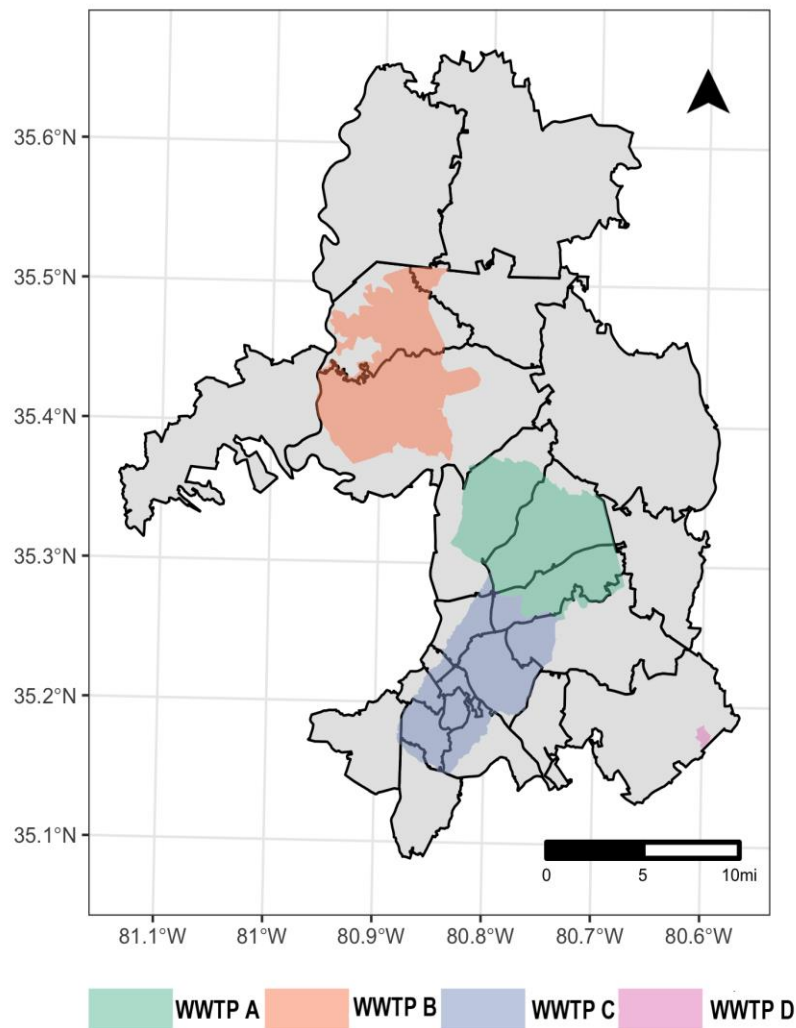
332 The average BCoV and HepG recovery efficiency for workflows 1 and 2 are provided in  
333 Supplementary Tables S2 and S3.

### 334 **2.6 Epidemiological data**

335 The North Carolina Department of Health and Human Services (NC DHHS) published the  
336 cumulative confirmed COVID-19 cases by 5-digit zip code as an online map  
337 (<https://nc.maps.arcgis.com/home/item.html?id=52f127a0767149ec984e91fcc06b06cb#overview>  
338 ). The map was typically updated daily, overwriting the previous day's count. We obtained a  
339 daily time series of cumulative cases from the WRAL online repository  
340 ([https://github.com/wraldata/nc-covid-data/tree/master/zip\\_level\\_data/time\\_series\\_data/csv](https://github.com/wraldata/nc-covid-data/tree/master/zip_level_data/time_series_data/csv)),  
341 which extracted and archived the NC DHHS published case reports each day. Missing counts in  
342 the WRAL archive were filled with the cumulative cases reported for the same date that we had  
343 manually archived from the NC DHHS COVID-19 dashboard for a subset of dates



344 (<https://covid19.ncdhhs.gov/dashboard/data-behind-dashboards>). We calculated daily incident  
345 cases as the difference between the current and previous day's reported cumulative cases,  
346 carrying the last non-missing value forward as necessary.  
347 Zip code and sewershed boundaries do not typically align (Fig.3). Daily case counts for each  
348 sewershed were represented by the sum of all cases in each zip code that substantially  
349 overlapped the sewershed boundary, defined as >50% of the zip code area within the sewershed  
350 or >50% of the sewershed area within the zip code. We used the 2019 American Community  
351 Survey (ACS) 5-year block group population estimates to estimate the population served by each  
352 sewershed.



353

354 **Fig.3.** Map showing the four sewershed location and the overlapping zip codes of Charlotte, NC.

## 355 **2.7 Statistical analysis**

356 Percent agreement statistics and Cohen's Kappa coefficient was used to determine the agreement  
357 of SARS-CoV-2 positivity and negativity results between the RT-qPCR and RT-ddPCR  
358 (McHugh, 2012; Obermeier et al., 2016). The strength of the agreement is interpreted based on  
359 the Kappa value (k): there is no agreement if  $k \leq 0$ , slight agreement if  $k = 0.01-0.20$ , fair if  $k =$   
360  $0.21-0.40$ , moderate if  $k = 0.41-0.60$ , substantial if  $k = 0.61-0.80$ , and nearly a perfect agreement  
361 if  $k = 0.81-1.00$  (McHugh, 2012). Spearman's rank correlation test was performed to determine  
362 the correlation of the SARS-CoV-2 concentration in influent wastewater with the averaged  
363 clinical (7-day moving average) COVID-19 cases. The correlation between the viral RNA signal  
364 and incident clinical cases, offset for 1 to 14 days (taking the wastewater influent collection date  
365 as the reference), was also computed for determining whether the influent wastewater SARS-  
366 CoV-2 RNA signal may serve as a leading indicator of the reported clinical cases. Case offset  
367 times exhibiting higher correlation with a p-value less than 0.05 were considered to be the  
368 probable lag time window.

## 369 **3. Results and discussion**

### 370 **3.1 RT-qPCR vs RT-ddPCR platform**

371 In this study, the utility of two different molecular platforms (RT-qPCR and RT-ddPCR)  
372 were compared to check SARS-CoV-2 detection frequency and concentration in the municipal  
373 influent wastewater.

#### 374 **3.1.1 Detection frequency and trends**

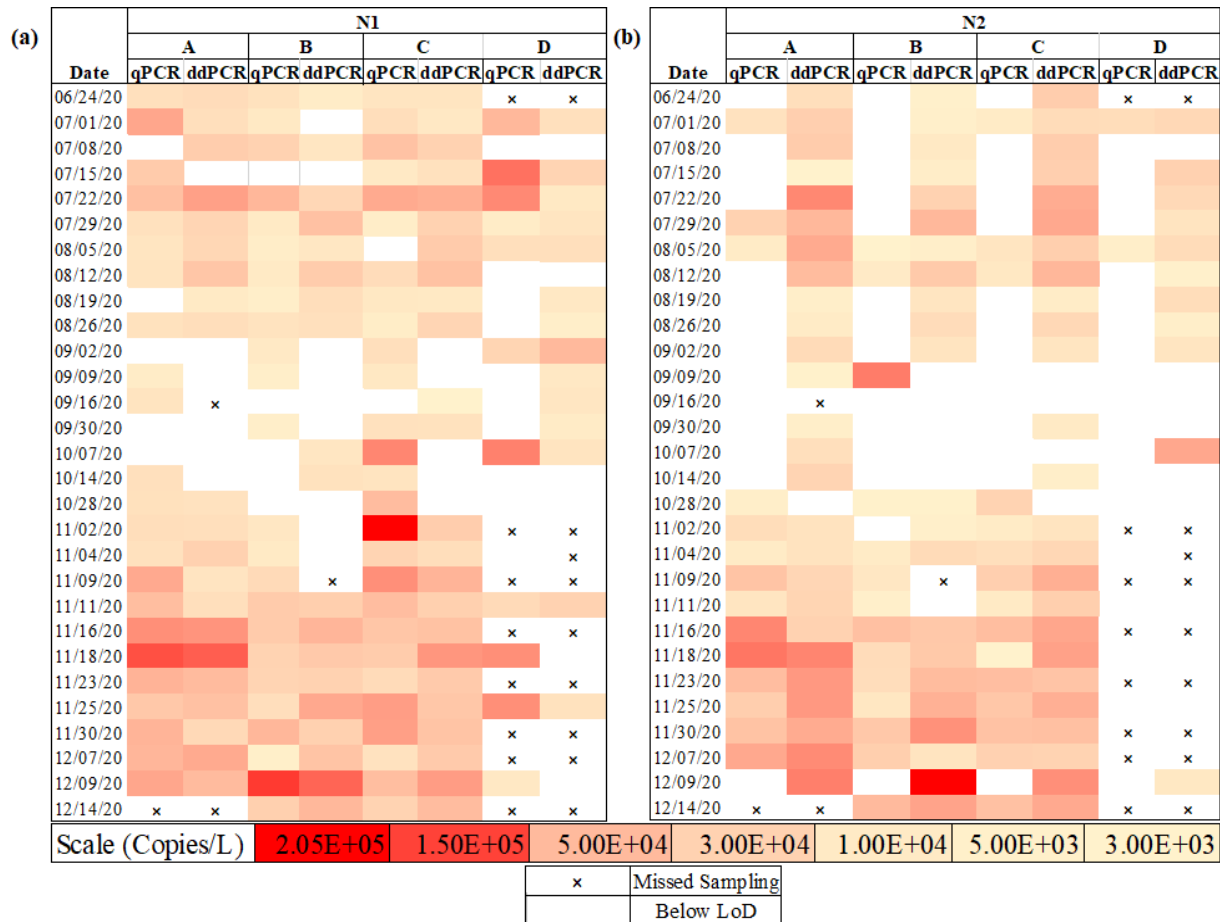
375 The detection frequency and trend of SARS-CoV-2 RNA in the municipal influent  
376 wastewater of Charlotte was observed by both RT-qPCR and RT-ddPCR using N1 and N2

377 targets. From the very first sampling event SARS-CoV-2 RNA was detected in the municipal  
378 wastewater influent samples of all the four WWTP throughout the six-month course (Fig. 4a).  
379 RT-qPCR detected a higher percentage of SARS-CoV-2 positives using the N1 target compared  
380 to N2 target (Table 3). About 27.83% of samples detected positive with the N1 target did not  
381 show any signal with the N2 target. In addition, the N2 assay showed inhibition while N1 did not  
382 (Table S4 and S5). On the other hand, RT-ddPCR performed well in detecting SARS-CoV-2  
383 using both N1 and N2 targets, though the N2 target was quantified in a higher percentage (36-  
384 48%) of samples (Table 3). When comparing the molecular platform, RT-ddPCR showed more  
385 sensitivity than RT-qPCR in quantifying SARS-CoV-2 RNA in wastewater samples. However,  
386 SARS-CoV-2 RNA was quantified more readily using the N1 target across all samples using  
387 both platforms. As such, downstream analysis was conducted only using N1 data. SARS-CoV-2  
388 positivity agreement between the two molecular platforms was 74.4% while the negative  
389 agreement was 52.6%. The overall percent agreement was 71% with the Cohen's Kappa  
390 coefficient (k) of 0.21. Ciesielski et al. (2021) also found a similar agreement with a k value of  
391 0.31 when comparing detection performance between RT-qPCR and RT-ddPCR. Other  
392 researchers compared RT-ddPCR and RT-qPCR and observed the former one to be more  
393 sensitive in the detection of low viral titer but they have mainly focused on N1 target only  
394 (Gonzalez et al., 2021).

395 **Table 3:** Detection frequency of N1 and N2 gene

WWTP	RT-qPCR		RT-ddPCR	
	N1 (%)	N2 (%)	N1 (%)	N2 (%)
A	82.14	50	77.8	96.3
B	82.75	48.3	67.9	78.6
C	93.1	51.72	82.76	86.2
D	55	10	73.68	57.9

396



397

398 **Fig.4.** Heat map of concentrations of (a) N1 and (b) N2 targets to evaluate SARS-CoV-2  
 399 prevalence at WWTP A, B, C and D using RT-qPCR and RT-ddPCR. The symbol “x” indicates  
 400 a missed sampling event and the uncolored blank spaces indicate a sample that was below the  
 401 limit of detection (LoD).

402

### 403 3.1.2 Quantitative relationship

404 The overall quantitative data generated using both RT-qPCR and RT-ddPCR for the WWTP A,  
 405 B, C was positively correlated ( $\rho=0.569$ ,  $p<0.0001$ ) with statistical significance. The agreement  
 406 between the platforms is shown using a range of colors corresponding to concentrations between  
 407 3.00E+03 copies/L and 2.05E+05 (Fig.4). RT-qPCR and RT-ddPCR generated similar SARS-  
 408 CoV-2 RNA concentration data across the duration of the study which is indicated by the  
 409 consistency between colors for both platforms on any given collection date. However, the

410 quantitative data of WWTP D was highly variable and not significantly correlated ( $\rho=-0.047$ ,  
411  $p=0.91$ ) which could be attributed to the fact that WWTP D is smaller in size and serves a  
412 smaller population compared to the other WWTP of Charlotte, NC. For most of the samples in  
413 this study, SARS-CoV-2 viral concentrations were in the range of  $10^3$ - $10^5$  copies/L for both RT-  
414 ddPCR and RT-qPCR. These SARS-CoV-2 concentrations are consistent with previous studies  
415 conducted by Sherchan et al. (2020) and Gonzalez et al. (2020) in wastewater throughout  
416 Louisiana and Southeastern Virginia, respectively. The highest peak value of SARS-CoV-2  
417 concentration in the influent wastewater for the WWTP A, B and C was observed to be around  
418  $1.15 \times 10^5$ - $1.96 \times 10^5$  copies/L by both RT-qPCR and RT-ddPCR. Also, the concentration of the  
419 88% quantified samples were within 0.5 log variation resulting in a percentage difference within  
420 12.5%. Miyani et al. (2020) also reported the highest SARS-CoV-2 concentration in the influent  
421 wastewater of Michigan to be within the range of  $2 \times 10^5$  copies/L. It is interesting to note that the  
422 highest viral quantification for both RT-ddPCR and RT-qPCR was observed by the end of  
423 November for WWTP A, B and C. Similar shades of colors (Fig. 4) were witnessed by the end of  
424 November indicating that the quantification by both RT-ddPCR and RT-qPCR were in  
425 agreement.

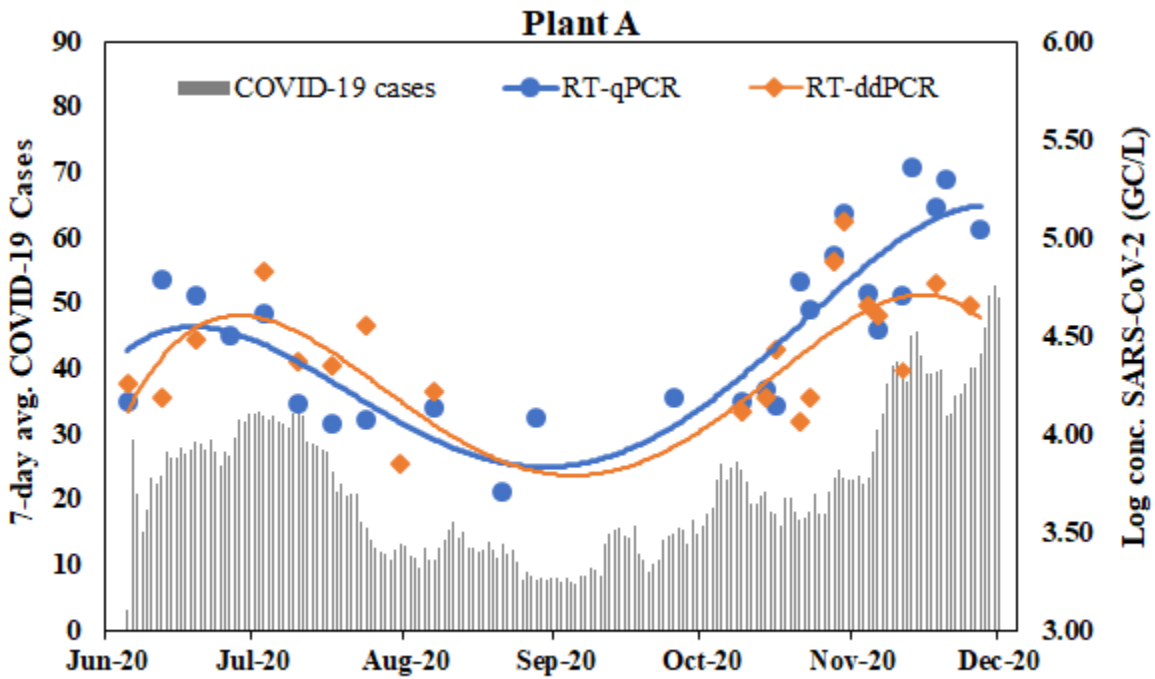
### 426 **3.2 COVID-19 clinical cases and SARS-CoV- 2 concentration in wastewater influent**

427 The concentration of SARS-CoV-2 in the municipal influent wastewater was correlated with the  
428 clinically reported COVID-19 case numbers for Mecklenburg County, Charlotte, NC. The  
429 SARS-CoV-2 concentration quantified by both RT-qPCR and RT-ddPCR in the influent  
430 municipal wastewater of Charlotte for all the WWTP were plotted against the clinically reported  
431 7-day average COVID-19 cases for zip codes served by each plant (Fig.5). From Fig. 5a, 5b and  
432 5c it is evident that the trends of reported COVID-19 cases match with the influent wastewater

433 concentration quantified by both RT-qPCR and RT-ddPCR. The influent wastewater  
434 concentration and the reported COVID-19 cases trends was a perfect match for WWTP A  
435 followed by WWTP C and B. For each WWTP, there was an increase during the summer months  
436 followed by a drop in both reported COVID-19 cases as well as influent wastewater  
437 concentration and then again, an increase was witnessed during the winter. In Charlotte, NC zip  
438 codes served by plants A and C mostly contributed to the increase in COVID-19 cases followed  
439 by WWTP B. Spearman rank correlation determined that there was a significant, moderate to  
440 strong, and positive correlation observed between SARS-CoV-2 RNA in influent wastewater and  
441 7-day average COVID-19 cases throughout the entirety of the six-month period. This correlation  
442 became more robust when clinically reported COVID-19 cases were lagged in against the  
443 influent wastewater SARS-CoV-2 data. With RT-qPCR, the influent wastewater SARS-CoV-2  
444 viral RNA data was likely to lead by 11 days ( $\rho=0.92$ ,  $p<0.001$ ), 10 days ( $\rho=0.81$ ,  $p<0.001$ ) and  
445 5 days ( $\rho=0.61$ ,  $p<0.001$ ) for WWTP A, B, and C, respectively while using RT-ddPCR, the lead  
446 time was 12 days ( $\rho=0.67$ ,  $p=0.001$ ), 7 days ( $\rho=0.72$ ,  $p<0.001$ ) and 10 days ( $\rho=0.50$ ,  $p<0.02$ )  
447 respectively. The lead time may vary depending on the sewershed pattern, the geospatial pattern  
448 of the population served for a WWTP, available testing facility and difference in the clinical  
449 sample collection date and result published to date (Bibby et al., 2021; Olesen et al., 2021). Even  
450 if the influent wastewater concentration data provided a predictive lead to the reported COVID-  
451 19 cases, it is interesting to note that the trend of the raw SARS-CoV-2 concentration data  
452 generated from the influent wastewater is similar to the reported COVID-19 cases. Additionally,  
453 SARS-CoV-2 concentration upsurge as quantified by both RT-qPCR and RT-ddPCR at a certain  
454 WWTP and decrease in another WWTP suggested that WBE provided us with the specific  
455 location where individuals are most or least infected than just the copies/L. Hasan et al. (2021)

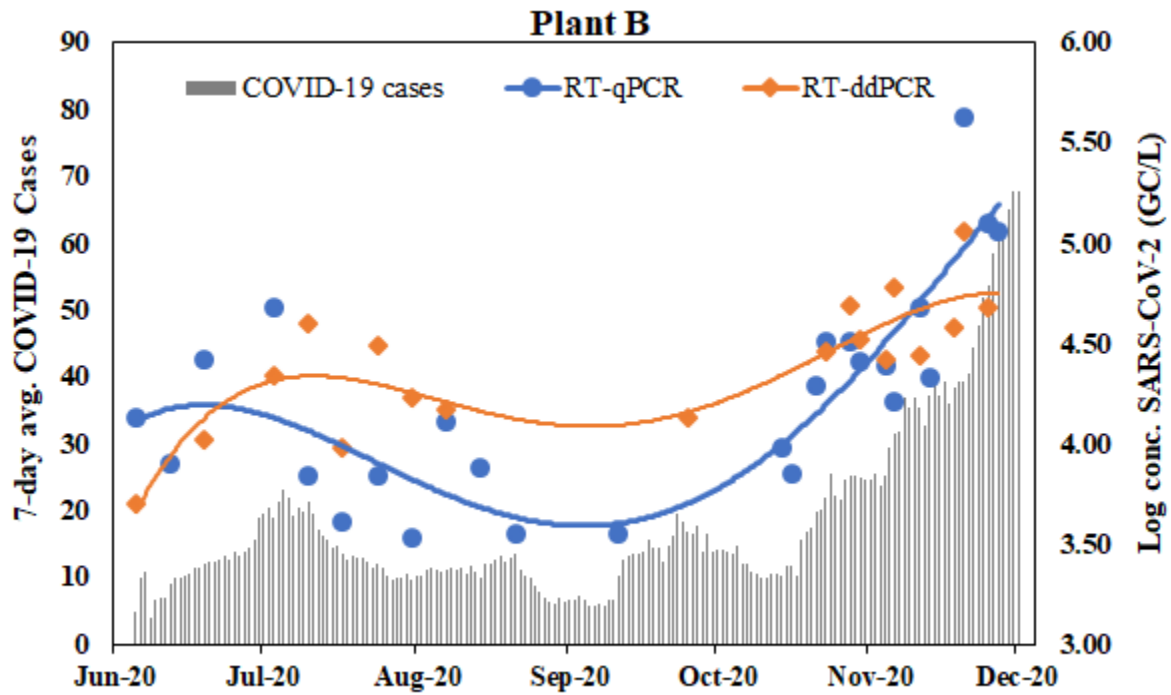
456 has also reported a similar observation where they have suggested the significant potential of  
457 WBE in monitoring upsurge or decline in COVID-19 positive case counts for a specific  
458 geographical location.

459 (a)



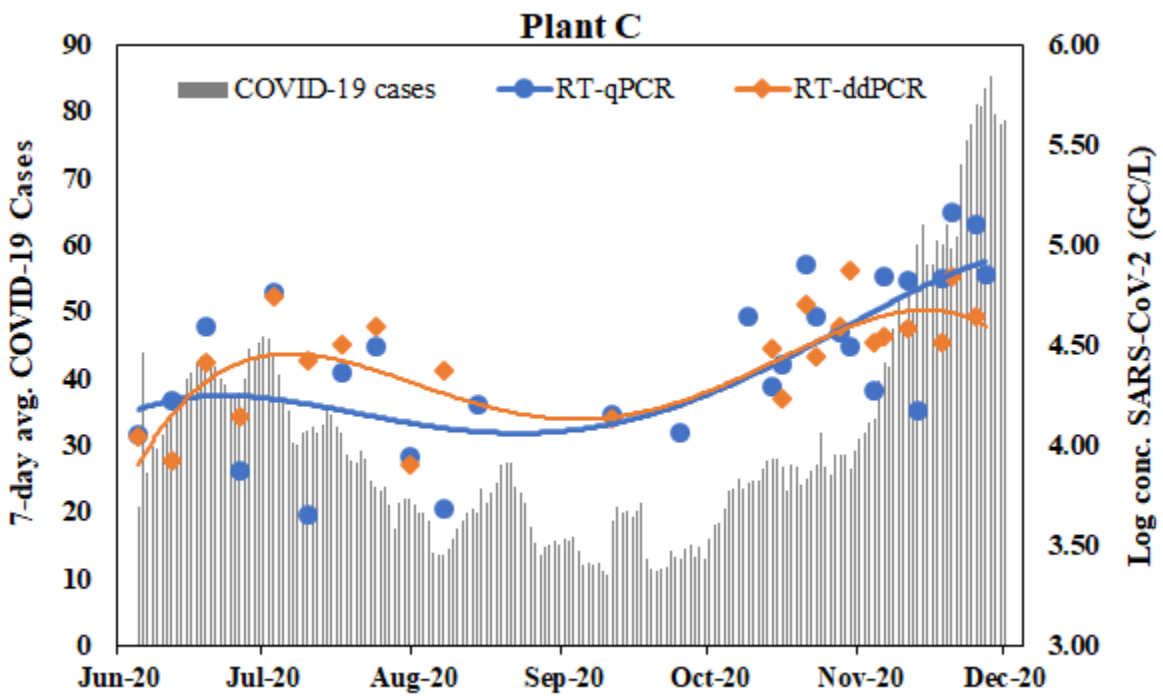
460

461 (b)



462  
463  
464

(c)



465



466 **Fig.5.** SARS-CoV-2 concentration (N1 target) for workflow 1 and 2 quantified by RT-qPCR and  
467 RT-ddPCR in the influent wastewater of (a) WWTP A, (b) WWTP B, and (c) WWTP C plotted  
468 against the 7-day average cases of each zipcode served by each WWTP. Quadratic polynomial  
469 trendline was used for the best fitted curve.

470

#### 471 **4. Conclusion**

472 This long-term monitoring study of WWTP in the Charlotte Metropolitan area has demonstrated  
473 that wastewater-based monitoring for the N1 target can be successfully carried out using either  
474 RT-qPCR or RT-ddPCR. Different molecular platforms didn't affect overall SARS-CoV-2  
475 quantification in the influent wastewater and showed a good agreement with a variation of less  
476 than 12.5% for most of the samples. Depending on the WWTP, the Spearman rank correlation  
477 showed a moderate to a strong positive correlation between the influent wastewater SARS-CoV-  
478 2 viral signal and 7-day averaged reported COVID-19 cases. Importantly, influent wastewater  
479 SARS-CoV-2 RNA signal strength was leading the reported clinical COVID-19 cases by 5 to 12  
480 days based on the WWTP, which is advantageous to monitor the COVID-19 outbreak in the  
481 community. Irrespective of the molecular platform used for the detection and quantification of  
482 SARS-CoV-2 in influent wastewater, it is important to incorporate all the QA/QC measures  
483 including implementation of appropriate external controls to obtain accurate and comparable  
484 results.

#### 485 **Acknowledgment**

486 This work was supported by North Carolina Policy Collaboratory. The authors acknowledge the  
487 support from the NC WW PATH team for early discussion and protocol sharing that was  
488 leveraged in this study. The authors would like to thank the Charlotte Water team including the  
489 wastewater treatment plant managers and operators for their support on wastewater sampling.

490 The authors are grateful to Stacie Reckling (NC DHHS) and Steven Berkowitz (NC DHHS) for  
491 help with sewershed boundaries and other site related logistics. The authors are also grateful to  
492 Vivek Francis Pulikkal for supporting sample collection and preparation of the NC map using  
493 ArcGIS Pro software and Sol Park for helping with initial sample collection.

#### 494 **References**

495 Agrawal, S., Orschler, L., & Lackner, S. (2021). Long-term monitoring of SARS-CoV-2 RNA in  
496 wastewater of the Frankfurt metropolitan area in Southern Germany. *Scientific Reports*, *11*(1),  
497 5372. <https://doi.org/10.1038/s41598-021-84914-2>

498 Ahmed, W., Angel, N., Edson, J., Bibby, K., Bivins, A., O'Brien, J. W., Choi, P. M., Kitajima,  
499 M., Simpson, S. L., Li, J., Tscharke, B., Verhagen, R., Smith, W. J. M., Zaugg, J., Dierens, L.,  
500 Hugenholtz, P., Thomas, K. V., & Mueller, J. F. (2020). First confirmed detection of SARS-  
501 CoV-2 in untreated wastewater in Australia: A proof of concept for the wastewater surveillance  
502 of COVID-19 in the community. *Science of the Total Environment*, *728*, 138764.  
503 <https://doi.org/10.1016/j.scitotenv.2020.138764>

504 Ahmed, W., Bertsch, P. M., Bibby, K., Haramoto, E., Hewitt, J., Huygens, F., Gyawali, P.,  
505 Korajkic, A., Riddell, S., Sherchan, S. P., Simpson, S. L., Sirikanchana, K., Symonds, E. M.,  
506 Verhagen, R., Vasan, S. S., Kitajima, M., & Bivins, A. (2020). Decay of SARS-CoV-2 and  
507 surrogate murine hepatitis virus RNA in untreated wastewater to inform application in  
508 wastewater-based epidemiology. *Environmental Research*, *191*(August), 110092.  
509 <https://doi.org/10.1016/j.envres.2020.110092>

510 Ahmed, W., Tscharke, B., Bertsch, P. M., Bibby, K., Bivins, A., Choi, P., Clarke, L., Dwyer, J.,  
511 Edson, J., Nguyen, T. M. H., O'Brien, J. W., Simpson, S. L., Sherman, P., Thomas, K. V.,  
512 Verhagen, R., Zaugg, J., & Mueller, J. F. (2021). SARS-CoV-2 RNA monitoring in wastewater

513 as a potential early warning system for COVID-19 transmission in the community: A temporal  
514 case study. *Science of the Total Environment*, 761, 144216.  
515 <https://doi.org/10.1016/j.scitotenv.2020.144216>

516 Albastaki, A., Najj, M., Lootah, R., Almeheiri, R., Almulla, H., Almarri, I., Alreyami, A., Aden,  
517 A., & Alghafri, R. (2021). First confirmed detection of SARS-COV-2 in untreated municipal and  
518 aircraft wastewater in Dubai, UAE: The use of wastewater based epidemiology as an early  
519 warning tool to monitor the prevalence of COVID-19. *Science of the Total Environment*, 760,  
520 143350. <https://doi.org/10.1016/j.scitotenv.2020.143350>

521 Aoust, P. M. D., Graber, T. E., Mercier, E., Montpetit, D., Alexandrov, I., Tariq, A., Mayne, J.,  
522 Zhang, X., Alain, T., Servos, M. R., Srikanthan, N., Mackenzie, M., Figeys, D., Manuel, D.,  
523 Jüni, P., Mackenzie, A. E., & Delatolla, R. (2021). *Science of the Total Environment Catching a*  
524 *resurgence : Increase in SARS-CoV-2 viral RNA identified in wastewater 48 h before COVID-*  
525 *19 clinical tests and 96 h before hospitalizations.* 770.  
526 <https://doi.org/10.1016/j.scitotenv.2021.145319>

527 Aoust, P. M. D., Mercier, E., Montpetit, D., Jia, J., Alexandrov, I., Neault, N., Tariq, A., Mayne,  
528 J., Zhang, X., Alain, T., Langlois, M., Servos, M. R., Mackenzie, M., Figeys, D., Mackenzie, A.  
529 E., Graber, T. E., & Delatolla, R. (2021). Quantitative analysis of SARS-CoV-2 RNA from  
530 wastewater solids in communities with low COVID-19 incidence and prevalence. *Water*  
531 *Research*, 188, 116560. <https://doi.org/10.1016/j.watres.2020.116560>

532 Bertrand, I., Challant, J., Mathieu, L., & Gantzer, C. (2021). *International Journal of Hygiene*  
533 *and Environmental Health Epidemiological surveillance of SARS-CoV-2 by genome*  
534 *quantification in wastewater applied to a city in the northeast of France : Comparison of*

535 *ultrafiltration- and protein precipitation-based metho.* 233(January).  
536 <https://doi.org/10.1016/j.ijheh.2021.113692>  
537 Bibby, K., Bivins, A., Wu, Z., & North, D. (2021). Making waves: Plausible lead time for  
538 wastewater based epidemiology as an early warning system for COVID-19. *Water Research*,  
539 202(July), 117438. <https://doi.org/10.1016/j.watres.2021.117438>  
540 Bivins, A., Greaves, J., Fischer, R., Yinda, K. C., Ahmed, W., Kitajima, M., Munster, V. J., &  
541 Bibby, K. (2020). *Persistence of SARS-CoV - 2 in Water and Wastewater*.  
542 <https://doi.org/10.1021/acs.estlett.0c00730>  
543 Bustin, S. A., Benes, V., Garson, J. A., Hellemans, J., Huggett, J., Kubista, M., Mueller, R.,  
544 Nolan, T., Pfaffl, M. W., & Shipley, G. L. (2009). *The MIQE Guidelines : M inimum I*  
545 *nformation for Publication of Q uantitative Real-Time PCR E xperiments SUMMARY : 622,*  
546 611–622. <https://doi.org/10.1373/clinchem.2008.112797>  
547 Cashdollar, J. L., & Wymer, L. (2013). *Methods for primary concentration of viruses from water*  
548 *samples : a review and meta-analysis of recent studies.* 1–11. <https://doi.org/10.1111/jam.12143>  
549 CDC. (2020). *03/10/2020: Lab Advisory: Updated Guidance on Testing Persons for*  
550 *Coronavirus Disease 2019 (COVID-19)*.  
551 [https://www.cdc.gov/csels/dls/locs/2020/updated\\_guidance\\_on\\_testing\\_persons\\_for\\_covid-](https://www.cdc.gov/csels/dls/locs/2020/updated_guidance_on_testing_persons_for_covid-19.html)  
552 [19.html](https://www.cdc.gov/csels/dls/locs/2020/updated_guidance_on_testing_persons_for_covid-19.html)  
553 Chik, A. H. S., Glier, M. B., Servos, M., Mangat, C. S., Pang, X. L., Qiu, Y., D'Aoust, P. M.,  
554 Burnet, J. B., Delatolla, R., Dorner, S., Geng, Q., Giesy, J. P., McKay, R. M., Mulvey, M. R.,  
555 Prystajecy, N., Srikanthan, N., Xie, Y., Conant, B., & Hruddy, S. E. (2021). Comparison of  
556 approaches to quantify SARS-CoV-2 in wastewater using RT-qPCR: Results and implications

557 from a collaborative inter-laboratory study in Canada. *Journal of Environmental Sciences*  
558 (*China*), 107, 218–229. <https://doi.org/10.1016/j.jes.2021.01.029>

559 Ciesielski, M., Blackwood, D., Clerkin, T., Gonzalez, R., Thompson, H., Larson, A., & Noble,  
560 R. (2021). Assessing sensitivity and reproducibility of RT-ddPCR and RT-qPCR for the  
561 quantification of SARS-CoV-2 in wastewater. *Journal of Virological Methods*, July, 114230.  
562 <https://doi.org/10.1016/j.jviromet.2021.114230>

563 Dumke, R., De, M., Barron, C., Oertel, R., Helm, B., Kallies, R., Berendonk, T. U., & Dalpke,  
564 A. (2021). *Evaluation of Two Methods to Concentrate SARS-CoV-2 from Untreated Wastewater*.  
565 1–7.

566 Gerrity, D., Papp, K., Stoker, M., Sims, A., & Frehner, W. (2021). Early-pandemic wastewater  
567 surveillance of SARS-CoV-2 in Southern Nevada: Methodology, occurrence, and  
568 incidence/prevalence considerations. *Water Research X*, 10, 100086.  
569 <https://doi.org/10.1016/j.wroa.2020.100086>

570 Gibas, C., Lambirth, K., Mittal, N., Islam, A., Bharati, V., Roppolo, L., Hinton, K., Lontai, J.,  
571 Stark, N., Young, I., Quach, C., Russ, M., Kauer, J., Nicolosi, B., Chen, D., Akella, S., Tang, W.,  
572 Schlueter, J., & Munir, M. (2021). Science of the Total Environment Implementing building-  
573 level SARS-CoV-2 wastewater surveillance on a university campus. *Science of the Total*  
574 *Environment*, 782, 146749. <https://doi.org/10.1016/j.scitotenv.2021.146749>

575 Gonçalves, J., Koritnik, T., Mio, V., Trkov, M., Bolje, M., Prosenc, K., Kotar, T., & Paragi, M.  
576 (2021). *Science of the Total Environment Detection of SARS-CoV-2 RNA in hospital wastewater*  
577 *from a low COVID-19 disease prevalence area*. 755, 4–10.  
578 <https://doi.org/10.1016/j.scitotenv.2020.143226>

579 Gonzalez, R. A., Larson, A., Thompson, H., Carter, E., & Cassi, X. F. (2021). Redesigning  
580 SARS-CoV-2 clinical RT-qPCR assays for wastewater RT-ddPCR. *MedRxiv*,  
581 2021.03.02.21252754. <https://doi.org/10.1101/2021.03.02.21252754>

582 Gonzalez, R., Curtis, K., Bivins, A., Bibby, K., Weir, M. H., Yetka, K., Thompson, H., Keeling,  
583 D., Mitchell, J., & Gonzalez, D. (2020). COVID-19 surveillance in Southeastern Virginia using  
584 wastewater-based epidemiology. *Water Research*, 186, 116296.  
585 <https://doi.org/10.1016/j.watres.2020.116296>

586 Graham, K. E., Loeb, S. K., Wolfe, M. K., Catoe, D., Sinnott-armstrong, N., Kim, S., Yamahara,  
587 K. M., Sassoubre, L. M., Grijalva, L. M. M., Roldan-hernandez, L., Langenfeld, K., Wigginton,  
588 K. R., & Boehm, A. B. (2021). SARS-CoV - 2 RNA in Wastewater Settled Solids Is Associated  
589 with COVID-19 Cases in a Large Urban Sewershed. *Environmental Science & Technology*.  
590 <https://doi.org/10.1021/acs.est.0c06191>

591 Haramoto, E., Malla, B., Thakali, O., & Kitajima, M. (2020). Science of the Total Environment  
592 First environmental surveillance for the presence of SARS-CoV-2 RNA in wastewater and river  
593 water in Japan. *Science of the Total Environment*, 737, 140405.  
594 <https://doi.org/10.1016/j.scitotenv.2020.140405>

595 Hasan, S. W., Ibrahim, Y., Daou, M., Kannout, H., Jan, N., Lopes, A., Alsafar, H., & Yousef, A.  
596 F. (2021). Science of the Total Environment Detection and quanti fi cation of SARS-CoV-2  
597 RNA in wastewater and treated ef fl uents : Surveillance of COVID-19 epidemic in the United  
598 Arab Emirates. *Science of the Total Environment*, 764, 142929.  
599 <https://doi.org/10.1016/j.scitotenv.2020.142929>

600 Hayden, R. T., Gu, Z., Ingersoll, J., Abdul-Ali, D., Shi, L., Pounds, S., & Caliendo, A. M.  
601 (2013). Comparison of droplet digital PCR to real-time PCR for quantitative detection of

602 cytomegalovirus. *Journal of Clinical Microbiology*, 51(2), 540–546.

603 <https://doi.org/10.1128/JCM.02620-12>

604 Hemalatha, M., Kiran, U., Kumar, S., Kopperi, H., Gokulan, C. G., Mohan, S. V., & Mishra, R.

605 K. (2021). Science of the Total Environment Surveillance of SARS-CoV-2 spread using

606 wastewater-based epidemiology : Comprehensive study. *Science of the Total Environment*, 768,

607 144704. <https://doi.org/10.1016/j.scitotenv.2020.144704>

608 Hillary, L. S., Farkas, K., Maher, K. H., Lucaci, A., Thorpe, J., Distaso, M. A., Gaze, W. H.,

609 Paterson, S., Burke, T., Connor, T. R., McDonald, J. E., Malham, S. K., & Jones, D. L. (2021).

610 Monitoring SARS-CoV-2 in municipal wastewater to evaluate the success of lockdown measures

611 for controlling COVID-19 in the UK. *Water Research*, 200, 117214.

612 <https://doi.org/10.1016/j.watres.2021.117214>

613 Juel, M. A. I., Stark, N., Nicolosi, B., Lontai, J., Lambirth, K., Schlueter, J., Gibas, C., & Munir,

614 M. (2021). Performance evaluation of virus concentration methods for implementing SARS-

615 CoV-2 wastewater based epidemiology emphasizing quick data turnaround. *Science of the Total*

616 *Environment*, 801, 149656. <https://doi.org/10.1016/j.scitotenv.2021.149656>

617 Kumar, M., Joshi, M., Patel, A. K., & Joshi, C. G. (2021). Unravelling the early warning

618 capability of wastewater surveillance for COVID-19: A temporal study on SARS-CoV-2 RNA

619 detection and need for the escalation. *Environmental Research*, 196(February), 110946.

620 <https://doi.org/10.1016/j.envres.2021.110946>

621 Kumar, M., Patel, A. K., Shah, A. V., Raval, J., Rajpara, N., Joshi, M., & Joshi, C. G. (2020).

622 First proof of the capability of wastewater surveillance for COVID-19 in India through detection

623 of genetic material of SARS-CoV-2. *Science of the Total Environment*, 746, 141326.

624 <https://doi.org/10.1016/j.scitotenv.2020.141326>

- 625 McHugh, M. L. (2012). Lessons in biostatistics interrater reliability : the kappa statistic.  
626 *Biochemica Medica*, 22(3), 276–282. <https://hrcak.srce.hr/89395>
- 627 Medema, G., Heijnen, L., Elsinga, G., Italiaander, R., & Medema, G. (2020). Presence of SARS-  
628 Coronavirus-2 in sewage . Methods Sewage samples. *MedRxiv*.  
629 <https://doi.org/https://doi.org/10.1101/2020.03.29.20045880>
- 630 Miyani, B., Fonoll, X., Norton, J., Mehrotra, A., & Xagorarakis, I. (2020). SARS-CoV-2 in  
631 Detroit Wastewater. *Journal of Environmental Engineering*, 146(11), 06020004.  
632 [https://doi.org/10.1061/\(asce\)ee.1943-7870.0001830](https://doi.org/10.1061/(asce)ee.1943-7870.0001830)
- 633 Murakami, M., Hata, A., Honda, R., & Watanabe, T. (2020). Letter to the Editor: Wastewater-  
634 Based Epidemiology Can Overcome Representativeness and Stigma Issues Related to COVID-  
635 19. *Environmental Science and Technology*, 54(9), 5311. <https://doi.org/10.1021/acs.est.0c02172>
- 636 Nemudryi, A., Nemudraia, A., Wiegand, T., Vanderwood, K. K., Wilkinson, R., Wiedenheft, B.,  
637 Nemudryi, A., Nemudraia, A., Wiegand, T., Surya, K., Buyukyoruk, M., & Cicha, C. (2020).  
638 Report Temporal Detection and Phylogenetic Assessment of SARS-CoV-2 in Municipal  
639 Wastewater II II Temporal Detection and Phylogenetic Assessment of SARS-CoV-2 in  
640 Municipal Wastewater. *Cell Reports Medicine*, 1(6), 100098.  
641 <https://doi.org/10.1016/j.xcrm.2020.100098>
- 642 Obermeier, P., Muehlhans, S., Hoppe, C., Karsch, K., Tief, F., Seeber, L., Chen, X., Conrad, T.,  
643 Boettcher, S., Diedrich, S., & Rath, B. (2016). Enabling Precision Medicine With Digital Case  
644 Classification at the Point-of-Care. *EBioMedicine*, 4, 191–196.  
645 <https://doi.org/10.1016/j.ebiom.2016.01.008>



646 Olesen, S. W., Imakaev, M., & Duvallet, C. (2021). Making waves: Defining the lead time of  
647 wastewater-based epidemiology for COVID-19. *Water Research*, 202, 117433.  
648 <https://doi.org/10.1016/j.watres.2021.117433>

649 Peccia, J., Zulli, A., Brackney, D. E., Grubaugh, N. D., Kaplan, E. H., Casanovas-massana, A.,  
650 Ko, A. I., Malik, A. A., Wang, D., Wang, M., Warren, J. L., Weinberger, D. M., Arnold, W., &  
651 Omer, S. B. (2020). Measurement of SARS-CoV-2 RNA in wastewater tracks community  
652 infection dynamics. *Nature Biotechnology*, 38(October). [https://doi.org/10.1038/s41587-020-](https://doi.org/10.1038/s41587-020-0684-z)  
653 0684-z

654 Pecson, B. M., Darby, E., Haas, C. N., Amha, Y. M., Bartolo, M., Danielson, R., Dearborn, Y.,  
655 Di Giovanni, G., Ferguson, C., Fevig, S., Gaddis, E., Gray, D., Lukasik, G., Mull, B., Olivas, L.,  
656 Olivieri, A., Qu, Y., & Sars-Cov-2 Interlaboratory Consortium. (2021). Reproducibility and  
657 sensitivity of 36 methods to quantify the SARS-CoV-2 genetic signal in raw wastewater:  
658 Findings from an interlaboratory methods evaluation in the U.S. *Environmental Science: Water*  
659 *Research and Technology*, 7(3), 504–520. <https://doi.org/10.1039/d0ew00946f>

660 Randazzo, W., Truchado, P., Cuevas-Ferrando, E., Simón, P., Allende, A., & Sánchez, G.  
661 (2020). SARS-CoV-2 RNA in wastewater anticipated COVID-19 occurrence in a low prevalence  
662 area. *Water Research*, 181. <https://doi.org/10.1016/j.watres.2020.115942>

663 Saguti, F., Magnil, E., Enache, L., Patzi, M., Johansson, A., Lumley, D., Davidsson, F., Dotevall,  
664 L., Mattsson, A., Trybala, E., Lagging, M., Lindh, M., Gisslén, M., Brezicka, T., Nyström, K., &  
665 Norder, H. (2021). *Surveillance of wastewater revealed peaks of SARS-CoV-2 preceding those of*  
666 *hospitalized patients with COVID-19*. 189. <https://doi.org/10.1016/j.watres.2020.116620>

667 Sherchan, S. P., Shahin, S., Ward, L. M., Tandukar, S., Aw, T. G., Schmitz, B., Ahmed, W., &  
668 Kitajima, M. (2020). Science of the Total Environment First detection of SARS-CoV-2 RNA in

669 wastewater in North America : A study in Louisiana , USA. *Science of the Total Environment*,  
670 743, 140621. <https://doi.org/10.1016/j.scitotenv.2020.140621>

671 Weidhaas, J., Aanderud, Z. T., Roper, D. K., Vanderslice, J., Brown, E., Ostermiller, J.,  
672 Hoffman, K., Jamal, R., Heck, P., Zhang, Y., Torgersen, K., Vander, J., & Lacross, N. (2021).  
673 Science of the Total Environment Correlation of SARS-CoV-2 RNA in wastewater with  
674 COVID-19 disease burden in sewersheds. *Science of the Total Environment*, 775, 145790.  
675 <https://doi.org/10.1016/j.scitotenv.2021.145790>

676 Westhaus, S., Weber, F., Schiwy, S., Linnemann, V., Brinkmann, M., Widera, M., Greve, C.,  
677 Janke, A., Hollert, H., Wintgens, T., & Ciesek, S. (2021). Science of the Total Environment  
678 Detection of SARS-CoV-2 in raw and treated wastewater in Germany – Suitability for COVID-  
679 19 surveillance and potential transmission risks. *Science of the Total Environment*, 751, 141750.  
680 <https://doi.org/10.1016/j.scitotenv.2020.141750>

681 WHO. (2020a). *Laboratory biosafety guidance related to coronavirus disease ( COVID-19 )*.  
682 *May*, 1–11.

683 WHO. (2020b). Responding to community spread of COVID-19. *Interim Guidance 7 March*,  
684 *March*, 1–6. [https://www.who.int/publications/i/item/responding-to-community-spread-of-covid-](https://www.who.int/publications/i/item/responding-to-community-spread-of-covid-19)  
685 19

686 Wurtzer, S., Marechal, V., Mouchel, J.-M., Maday, Y., Teyssou, R., Richard, E., Almayrac, J. L.,  
687 & Moulin, L. (2020). Evaluation of lockdown impact on SARS-CoV-2 dynamics through viral  
688 genome quantification in Paris wastewaters. *MedRxiv*, 2020.04.12.20062679.  
689 <https://doi.org/10.1101/2020.04.12.20062679>

- 690 Yan Bai, Yao, L., TaoWei, Tian, F., Jin, D.-Y., Chen, L., & MeiyunWang. (2020). Presumed  
691 Asymptomatic Carrier Transmission of COVID-19. *JAMA*, 382(13), 1199–1207.  
692 <https://doi.org/10.1056/nejmoa2001316>
- 693 Zhao, L., Atoni, E., Nyaruaba, R., Du, Y., Zhang, H., Donde, O., Huang, D., Xiao, S., Ren, N.,  
694 Ma, T., Shu, Z., Yuan, Z., Tong, L., & Xia, H. (2021). Environmental surveillance of SARS-  
695 CoV-2 RNA in wastewater systems and related environments in Wuhan : April to May of 2020.  
696 *Journal of Environmental Sciences*, 0–17. <https://doi.org/10.1016/j.jes.2021.05.005>  
697

